CRYSTAL GROWTH & DESIGN

Article

pubs.acs.org/crystal

Interactions of Aromatic Residues in Amyloids: A Survey of Protein Data Bank Crystallographic Data

Ivana M. Stanković,[†] Dragana M. Božinovski,[‡] Edward N. Brothers,[§] Milivoj R. Belić,[§] Michael B. Hall,[∥] and Snežana D. Zarić*[,‡,§]

[†]Institute of Chemistry, Technology and Metallurgy, University of Belgrade, Njegoševa 12, 11000 Belgrade, Serbia

[‡]Department of Chemistry, University of Belgrade, Studentski trg 12-16, 11000 Belgrade, Serbia

[§]Science Program, Texas A&M University at Qatar, Texas A&M Engineering Building, Education City, Doha, Qatar

[∥]Department of Chemistry, Texas A&M University, College Station, Texas 77843-3255, United States

Supporting Information

ABSTRACT: Aromatic−aromatic interactions have long been considered important in the self-assembly of amyloids. In spite of their importance, aromatic amino acids are not detected in every amyloid. In the present study, the occurrence and geometry of these interactions were analyzed for the amyloid structures found in the Protein Data Bank. The data confirm that aromatic amino acids are not crucial for amyloid fibril formation. In fact, aromatic−aliphatic interactions are more frequent than the aromatic−aromatic interactions. Aromatic−aliphatic interactions are present in higher numbers of structures and in certain amyloid sequences; they are more frequent than aromatic−aromatic interactions. An analysis of aromatic/aromatic interactions shows different interaction geometries in intrasheet and intersheet contacts; the intrasheet aromatic−aromatic interactions are mostly parallel and displaced, while intersheet interactions are not parallel. Thus, among the aromatic−aromatic interactions there are important edge-to-face attractions in addition to parallel stacking ones.

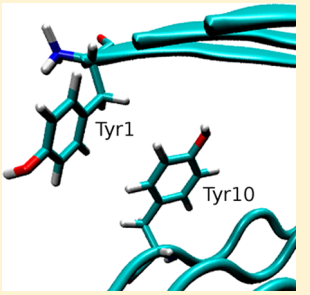

INTRODUCTION

Amyloids are insoluble proteins of a cross-β structure found as deposits in many neurodegenerative diseases, such as Alzheimer's, Parkinson's, Creutzfeldt−Jakob's, Huntington's, or in type II diabetes.[1−6] Because of their strong fibrillar nature, they can be found in normal tissues as well, like nails, spider webs, or silk.[7] Amyloids have attracted great attention because of their perceived role in various diseases, unique architecture, and exceptional physical properties.[6,8] Short polypeptides, with a minimum length of four amino acids, are self-assembled into β-sheets via backbone hydrogen bonds, and then several β-sheets interact with each other via polypeptide side chains, to form long linear unbranched protofilaments with an axis nearly perpendicular to a polypeptide strand.[9] Several protofilaments, the number being specific to the particular amyloid protein, form fibrils.[10] All amyloid proteins, independent of their sequence, form similar structures, namely, the cross-β structure which is made of parallel arrays of β-strands. These structures differ only in the intersheet spacing, which depends on the side chain size, and in the morphology of a fibril.[10]

Although they are not indispensable, the aromatic amino acids phenylalanine (Phe), tyrosine (Tyr), and tryptophan (Trp) appear to be important in amyloid formation, kinetics, and thermodynamic stability.[9,11−22] Aromatic amino acids are hydrophobic and have a high β-sheet propensity. These properties appear crucial in amyloid formation. Furthermore, aromatic amino acids possess an ability to engage in $\pi-\pi$ interactions and have a directing role in the kinetics of amyloid formation.[9,10,12,14,15,23]

Aromatic−aromatic interactions (Ar/Ar) generally give rise to three different types of geometries that differ by the angle between rings and offset values: edge-to-face/T-shaped, face-to-face, and parallel displaced (offset stacked) interactions (Figure 1). Generally, the face-to-face orientation is rarely observed, as it leads to an unfavorable electrostatic repulsion between the two planar faces of the aromatic rings. The majority of interactions in the proteins in general fall into a T-shaped orientation.[24−26]

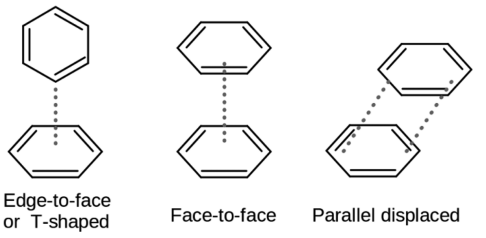

Figure 1. Representation of the three aromatic−aromatic interaction types.

Received: July 25, 2017
Revised: October 19, 2017
Published: October 23, 2017

DOI: 10.1021/acs.cgd.7b01035
Cryst. Growth Des. XXXX, XXX, XXX−XXX

Our previous work based on the analysis of crystal structures from the Cambridge Structural Database (CSD), protein structures from the Protein Data Bank (PDB), and quantum chemical calculations showed the importance of parallel aromatic−aromatic interactions at large offsets of 4.5−5.5 Å.[26,27] The quantum chemical calculations indicate that even at large offsets, the stacking interactions are quite strong, with an interaction energy of −2.0 kcal/mol.[27]

Our recent quantum chemical calculations[28] of pairs of amyloid β-sheets indicate that the aromatic−aliphatic interactions contribute the most to amyloid stability, in the case of amyloids with aromatic amino acids, while aliphatic−backbone interactions contribute the most to amyloid stability in the case of aliphatic amyloids (amyloids without aromatic residues). These results also support previous findings that amyloid β-structures can be formed by nonaromatic peptides. Also, our calculations of cyclohexane−benzene[31] and benzene−benzene[27] interactions indicate stronger aromatic−aliphatic interactions than the aromatic−aromatic ones.

In several studies, $\pi-\pi$ interactions in amyloids were detected through indirect experimental methods, like UV fluorescence spectroscopy,[28] circular dichroism,[11,30] and the importance of these interactions in amyloid aggregations was assessed without any atomic level characterization.

In the present study, a systematic investigation of interactions of aromatic side chains at atomic resolution was performed by using X-ray and NMR structures of amyloids deposited in the PDB. Both natural and synthetic amyloids were included in the study, by taking only cross-β and parallel coil structures into account, in a thorough search of PDB for amyloids. Since fibril growth can be conducted through β-sheet by increasing the hydrogen bonding between β-strands within the same β-sheet, or by side chain interactions between different β-sheets,[10] these two types of Ar/Ar interactions were distinguished as intrasheet and intersheet (Figure 2). To the best of our knowledge, this is the first systematic study of interactions of aromatic side chains in all amyloid structures deposited in the PDB.

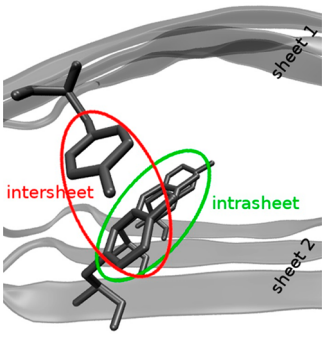

Figure 2. Example of intrasheet and intersheet contacts in an amyloid protein, PDB ID 2NNT.

MATERIALS AND METHODS

PDB Database. Amyloid protein three-dimensional (3D) structures were searched in the PDB[31] and in the CSD.[32] The searching criterion for the CSD was any at least four residue long acyclic polypeptide with a nearly β-sheet structure. Eight structures were found, but with no proof of self-assembly in the published papers. An amyloid PDB subdatabase was made by searching the PDB for an amyloid precursor name in the case of natural amyloids, and for the terms *amyloidogenic*, *amyloid-related*, and *amyloid-like* for synthetic amyloids. Only the β secondary structures or coils were taken into account. The details of the procedure for the database search have been explained previously.[33] There were 109 structures found in the PDB that fit these criteria, resolved by X-ray crystallography, solid state or solution NMR. Some NMR structures are multiframe with up to 20 conformers, so total of 303 conformers were analyzed. There are 83 different peptide sequences in the constructed database. The X-ray structures have been translated and rotated in order to obtain full crystal lattice and biological assembly defined in PDB files; after, duplicate interactions and amino acids have been excluded. In order to determine the occurrence and impact of aromatic rings, all interactions of aromatic rings, both aromatic−aromatic (Ar/Ar) and aromatic−nonaromatic (Ar/nAr), were analyzed in every one of these sequences.

Aromatic−Aromatic Interactions. All the combinations of interactions between the three aromatic amino acids, Phe, Tyr, and Trp, were taken into account. Histidine was not taken into consideration because it can be charged and thus screen more delicate $\pi-\pi$ interaction. For Trp, we considered interactions of the six-membered ring, while we did not consider interactions of the five-membered ring. We determined the center−center distance between the rings (d), the angle between ring planes (P_1/P_2), the normal distance between ring planes (R), and the offset between ring centers (r), shown in Figure 3. The distance (R) represents the normal

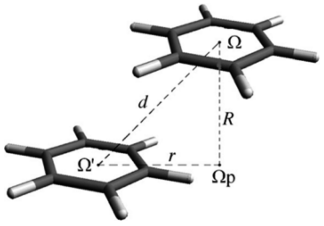

Figure 3. Geometric parameters determined for each PDB amyloid structure: the center−center distance between rings (d), the angle between ring planes (P_1/P_2), the normal distance between planes (R), the offset between ring centers (r).

distance of the center of one ring (Ω) to its projection onto the plane of the other ring (Ω_p). The horizontal displacement (offset) r represents the distance of the center of one ring (Ω') to the projection of the center of the other ring onto the plane of the first ring (Ω_p). For (P_1/P_2) angles other than zero, there are two alternative and unequal pairs of R and r; we have used the higher R and its corresponding r value, as in ref 26. The distances between the Cα atoms of two interacting amino acids have been calculated as well. The scripts for the search and for the PDB file parsing were written in Python (http://www.python.org/) by using the MDAnalysis python library.[34] Duplicate interactions have been recognized as having the same d distance and excluded.

Aromatic molecules can form other types of interactions as well, such as C−H/O and C−H/π. A contact was considered C−H/O interaction if the distance between a hydrogen atom from the C−H group of an amino acid and an oxygen atom from another amino acid was less than 2.9 Å and the C−H−O angle larger than 110°.[35,36] The geometrical criteria for the C−H/π interaction were the distance between the H atom and the center of phenyl ring is shorter than 3.5 Å, the angle between the C−H vector and the phenyl ring center is in the range 110−180°, and the angle between the vector H atom—center of the ring and the vector normal to the ring is smaller than 30°.[37]

We also distinguished Ar/Ar interactions when the aromatic rings pertain to parallel and antiparallel strand, by defining angle between vectors C−Cα for the two residues. When this vector was less than 90°, the strands were considered parallel.

Aromatic−Nonaromatic Interactions. To describe the Ar/nAr interactions, the minimum distance between heavy atoms of two interacting amino acids was calculated, taking into consideration side chains only. The backbone interactions were not considered, as they

DOI: 10.1021/acs.cgd.7b01035
Cryst. Growth Des. XXXX, XXX, XXX−XXX

Table 1. Number and Percentages of Aromatic Amino Acids in Amyloid Sequences and Structures, and Their Involvement in Aromatic−Aromatic or Aromatic−Nonaromatic Interactions[a]

	no. sequences with aromatics		no. aromatics in sequences		no. structures with aromatics		no. aromatics in structures		no. aromatics involved in Ar/Ar				no. aromatics involved in Ar/nAr			
									intersheet		intrasheet		intersheet		intrasheet	
Phe	38	45.8%	54	55.1%	48	44.0%	3505	57.1%	171	2.8%	2663	43.4%	2759	45.0%	387	6.3%
Tyr	32	38.6%	40	40.8%	49	45.0%	2351	38.3%	670	10.9%	1210	19.7%	723	11.8%	403	6.6%
Trp	3	3.6%	4	4.1%	5	4.6%	280	4.6%	61	1.0%	155	2.5%	164	2.7%	89	1.5%
total	56	67.5%	98		78	71.6%	6136		902	14.7%	4028	65.6%	3646	59.4%	879	14.3%

[a]Ar/Ar = aromatic−aromatic interactions, Ar/nAr = aromatic−nonaromatic interactions. There are 83 sequences and 109 structures in total.

Table 2. Number and Percentages of Structures and Interactions Involving Aromatic Amino Acids[a]

		no. structures				no. interactions			
		intersheet		intrasheet		intersheet		intrasheet	
Ar/Ar	PhePhe	7	6.4%	21	19.3%	10	2.4%	1492	64.6%
	PheTyr	2	1.8%	0	0.0%	3	0.7%	0	0.0%
	PheTrp	0	0.0%	1	0.9%	0	0.0%	4	0.2%
	TyrTyr	14	12.8%	15	13.8%	397	96.8%	797	34.5%
	TrpTrp	0	0.0%	1	0.9%	0	0.0%	16	0.7%
	total	21	19.3%	33	30.3%	410		2309	
Ar/nAr	Phe	48	44.0%	33	30.3%	6902	72.4%	877	43.6%
	Tyr	48	44.0%	31	28.4%	1827	19.2%	963	47.9%
	Trp	4	3.7%	5	4.6%	810	8.5%	170	8.5%
	total	78	71.6%	51	46.8%	9539		2010	

[a]Ar/Ar = aromatic−aromatic interactions, Ar/nAr = aromatic−nonaromatic interactions. Total number of structures is 109, 78 of which contain aromatic amino acids.

are not specific to an amino acid. The minimum distance between heavy atoms was limited to 5.0 Å in the search, as the sum of van der Waals radii never exceeds this value, according to the CHARMM parameters.[38] The interactions were discriminated as intersheet with the Cα−Cα distance > 8 Å, and intrasheet with Cα−Cα distance < 6 Å, according to the results for the Ar/Ar. One interaction was counted as one pair of residues.

Number of Rings Involved in Interactions. The number of aromatic amino acids taking part in Ar/Ar or exclusively Ar/nAr interactions was determined in every amyloid structure. An Ar/Ar interaction was defined within the area that corresponds to the ellipse (r = 7.0 Å and R = 6.0 Å) according to the results for the Ar/Ar search. Ar/nAr interactions were defined as maximum heavy atom−heavy atom distance up to 5.0 Å, according to the Ar/nAr search.

RESULTS AND DISCUSSION

We searched and analyzed interactions of aromatic side chains in the subdatabase formed by amyloid structures deposited in the PDB from June 2016. In the PDB, 83 sequences and 109 amyloid structures were found, while 67.5% sequences and 71.6% structures contain aromatic amino acids (Table 1). These data show that amyloid structures can exist without aromatic amino acids, as was observed previously.[9] Moreover, in a number of structures with aromatic amino acids, the Ar/Ar interactions do not exist; among 109 structures, the Ar/Ar interactions were observed only in 48 structures, and specifically intesheet Ar/Ar interactions are present only in 21 structures (19.3%, Table 2). Hence, our data confirm that neither aromatic amino acids nor Ar/Ar interactions are crucial for amyloid existence.

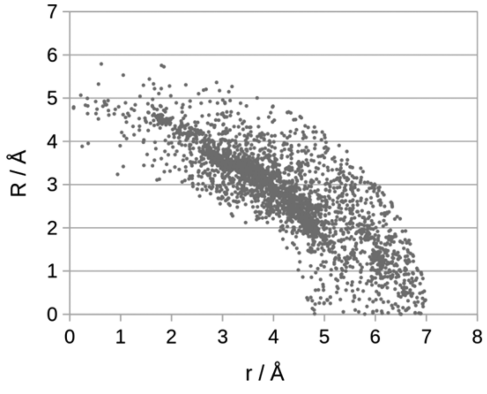

Figure 4. Normal distance (R) dependence on the offset values (r).

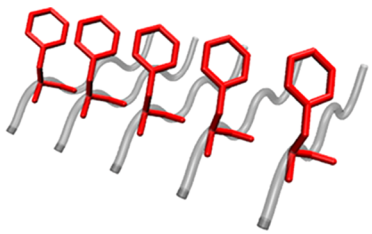

Figure 5. Example of the most frequent geometrical arrangement of the intrasheet interactions. PDBid: 4R0P, P_1/P_2 = 0.0°, r = 3.57 Å.

The analysis has been done separately for the amino acids Phe, Tyr, and Trp, in order to detect different substituents influences. The occurrence of aromatic amino acids among all amino acids in amyloids is 3.92% for Phe, 2.90% for Tyr and 0.29% for Trp, which is very similar to the occurrences in general protein sequences taken from Uniprot,[39] for Phe and Tyr (3.93% and 2.94%, respectively), while occurrence for Trp is larger in general protein sequence, 1.29%.

As was mentioned above, the intersheet and intrasheet interactions were analyzed separately. The intrasheet Ar/Ar interactions are far more frequent than the intersheet ones (2309 over 410, Table 2), and also a higher number of rings is

DOI: 10.1021/acs.cgd.7b01035
Cryst. Growth Des. XXXX, XXX, XXX−XXX

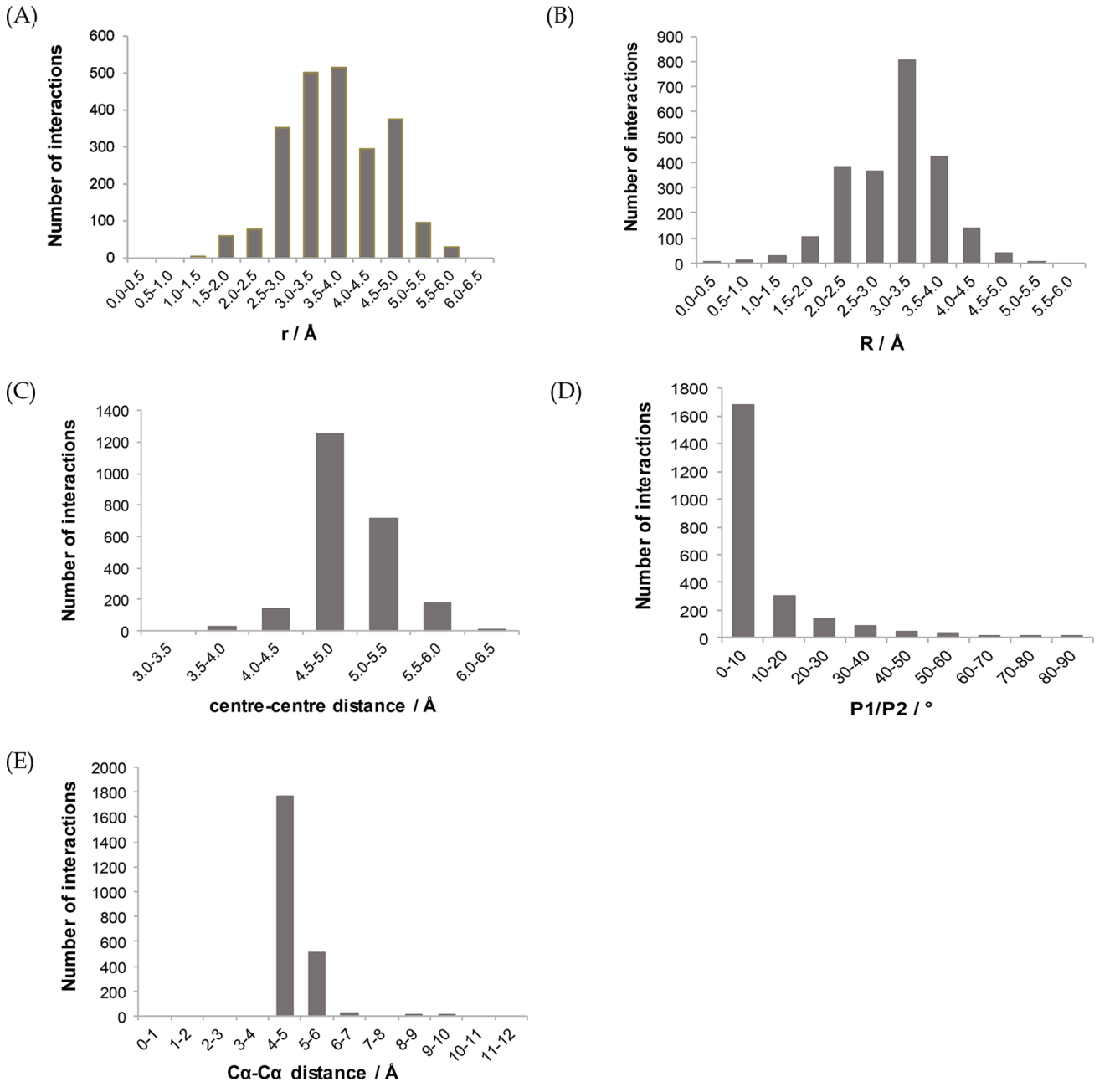

Figure 6. Geometrical parameters for the intrasheet aromatic−aromatic interactions: (A) Distribution of the offset values (r), (B) distribution of the normal distances (R), (C) center−center distance distribution, (D) distribution of the angle between aromatic rings, and (E) distribution of the Cα−Cα distances.

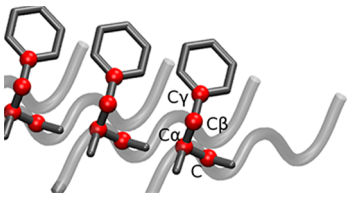

Figure 7. Torsion angle T of an aromatic amino acid between the atoms C, Cα, Cβ, and Cγ.

involved in the intrasheet interactions (4028 over 902, Table 1).

Considering intersheet interactions, the data in Table 1 show that the number of aromatic amino acids involved in Ar/nAr interactions (3646) is larger than the number of aromatic amino acids involved in Ar/Ar interactions (902). Also, the number of Ar/nAr interactions (9539) is larger than the number of Ar/Ar interactions (410), as data in Table 2 indicate. On the other hand, for the intrasheet interactions, the Ar/Ar (2309) are more preferred than the Ar/nAr ones (2010, Table 2), and also a higher number of rings is involved in Ar/Ar (4028) than in Ar/nAr (879, Table 1).

Aromatic−Aromatic Interactions. The common characteristic of all the Ar/Ar interactions found in amyloid PDB structures is that the normal distance between rings (R) decreases as the offset value increases (r), as seen in Figure 4. The database search yielded 3573 contacts found to be within

DOI: 10.1021/acs.cgd.7b01035
Cryst. Growth Des. XXXX, XXX, XXX−XXX

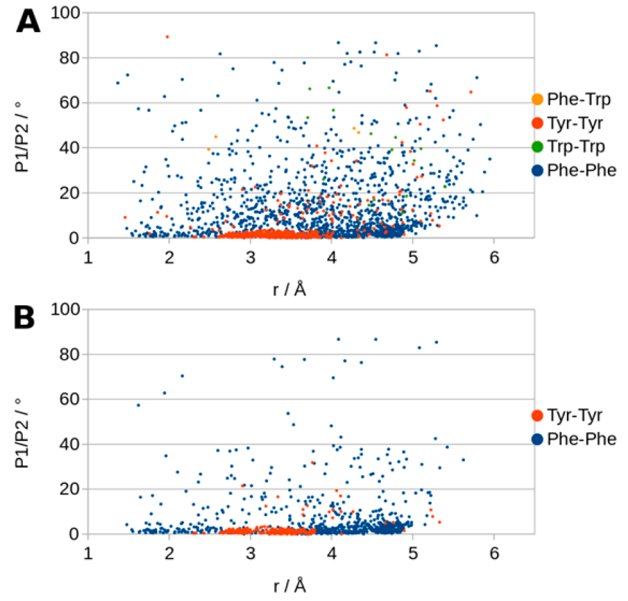

Figure 8. P_1/P_2 angle-offset dependence for intrasheet aromatic−aromatic interactions. Different amino acid pairs represented in various colors. (A) P_1/P_2 (offset) function for all intrasheet interactions. (B) P_1/P_2 (offset) function for intrasheet interactions not exposed to the solvent.

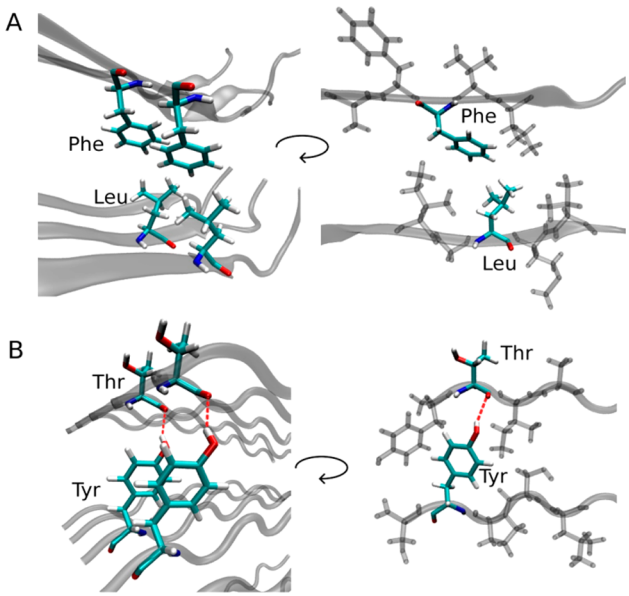

Figure 9. Intrasheet aromatic−aromatic interactions. (A) Type Phe−Phe exhibits higher offset values (right), PDB ID 2LMQ, r = 4.95 Å. (B) Type Tyr−Tyr exhibits lower offset values (right), PDB ID 2M5K, r = 2.30 Å. Besides intraseet $\pi-\pi$ interactions between aromatic rings, Phe and Tyr residues have additional interactions with the opposite amyloid sheet. Phenylalanines interact through their π-cloud with hydrophobic residues in the surrounding (Leu, C−H/π interaction), while tyrosines form hydrogen bonds with the opposite sheet backbone through their −OH group, O−H−O angle 155.24°, O−O distance 3.41 Å.

the area that corresponds to the ellipse (r = 7.0 Å and R = 6.0 Å).

Some longer amyloid peptides exhibit the structure of a β-turn-β and look like U-shaped β-sheets. The aromatic rings contained in these unstructured turns, as well as in the unstructured β-strand extremities, were not accounted for in the interaction analysis, as they do not give rise to the cross-β amyloid structure (Figure S1). In other words, only the interacting cross-β fragments were analyzed in this study, and hence we analyzed 2719 interactions. The geometric parameters were analyzed separately for the intersheet and the intrasheet Ar/Ar interactions.

Intrasheet Aromatic−Aromatic Interactions. When it comes to the intrasheet arrangements, more than two aromatic rings are stacked, and the rings are arranged in a nearly parallel orientation, with varying offset values. The structure in Figure 5 represents one typical example of these structural motifs. The data on geometries of these interactions are given in Figure 6, where the characteristic angles between ring planes, P_1/P_2, are 0−5° and the offset values (r) are in the range 2.5−5.0 Å. The Cα−Cα distance is in a small range, since it corresponds to the intrasheet distances and is a general property of proteins, about ∼4.7 Å.[10] As the distance between two amino acids is constant, the variation in the center−center distance between rings (d) and in the offset value (r) (Figure 6) is due to the change in the torsion angle C−Cα−Cβ−Cγ, presented in Figure 7.

In order to probe the influence of the ring type, the P_1/P_2 angle-offset dependence was separately shown for the four systems, Phe−Phe, Phe−Trp, Tyr−Tyr, and Trp−Trp, which were found in the interactions involving combinations of three aromatic amino acids (Figure 8A). All systems, except Trp−Trp, show a tendency toward parallel interactions, and a large range of offset values. The systems with tryptophan exhibit less parallel geometries, which could be the consequence of a small number of these interactions (Table 2). Namely, all the Trp−Trp interactions were found in one 10-framed NMR structure, and all tryptophans were positioned toward the water environment with higher conformational freedom (Figure S2).

In the polar solvent environment, the dielectric constant is higher than in the hydrophobic core of proteins, and the polar interactions screen the delicate $\pi-\pi$ interactions. Hence, Figure 8B presents the P_1/P_2 angle-offset dependence when all intrasheet interactions with aromatic rings that are close to the water environment are excluded. The comparison of data in Figure 8A,B shows that the interactions in the polar solvent environment have high P_1/P_2 angles and can have high offset values. The interactions in the hydrophobic core show tendencies toward smaller P_1/P_2 angles (Figure 8B). One can notice that only Phe−Phe and Tyr−Tyr interactions occur in the hydrophobic core.

In comparison to tyrosine aromatic rings, the phenylalanine rings demonstrate a higher tendency to form intrasheet Ar/Ar interactions with a larger range of offset values and large range of inter-ring angles (Figure 8B). Visual inspection of the amyloid structures indicated that Phe rings are found nearly parallel to the sheet plane, while the Tyr rings point toward the opposite amyloid sheet, as presented in the examples in Figure 9. Tyr possesses the −OH group and can form hydrogen bonds with the opposite sheet backbone (Figure 9B); this is the reason why offset values for Tyr−Tyr interactions are in a relatively small range, and they have a small angle P_1/P_1 (almost parallel interactions, Figure 8). Hence, hydrogen bonds of −OH group of tyrosine with the opposite backbone are responsible for different geometries in Phe−Phe and Tyr−Tyr contacts.

Phenylalanine residues that form interactions at large offsets (3.5−5.0 Å) can form simultaneous interactions with ring faces. It was previously demonstrated that high offsets in phenyl−

DOI: 10.1021/acs.cgd.7b01035
Cryst. Growth Des. XXXX, XXX, XXX−XXX

Table 3. Number and Percentages of Intersheet and Intrasheet Aromatic−Nonaromatic Interactions between Different Aromatic and Nonaromatic Residues[a]

intersheet Ar/nAr							intrasheet Ar/nAr						
	Phe		Tyr		Trp			Phe		Tyr		Trp	
Leu	2018	21.2%	154	1.6%	185	1.9%	Val	266	13.2%	314	15.6%	0	0.0%
Ile	1556	16.3%	450	4.7%	0	0.0%	Ser	32	1.6%	338	16.8%	0	0.0%
Val	759	8.0%	300	3.1%	33	0.3%	Glu	218	10.8%	128	6.4%	0	0.0%
Ala	757	7.9%	77	0.8%	0	0.0%	Asp	48	2.4%	9	0.4%	116	5.8%
Glu	585	6.1%	105	1.1%	126	1.3%	Leu	155	7.7%	17	0.8%	0	0.0%
Asn	599	6.3%	173	1.8%	11	0.1%	Ala	83	4.1%	61	3.0%	1	0.0%
Arg	174	1.8%	20	0.2%	294	3.1%	Thr	6	0.3%	39	1.9%	21	1.0%

[a]The most frequent interactions are represented. Total number of the interactions is 9539 for the intersheet and 2010 for the intrasheet interactions.

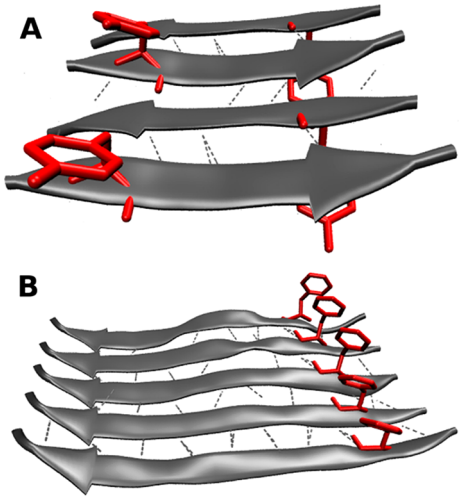

Figure 10. (A) Antiparallel beta-sheet arrangement prevents the intrasheet aromatic−aromatic interactions, PDB ID 3MD4, and (B) parallel arrangement results in the intrasheet interactions, PDB ID 2BEG. Dashed lines represent the backbone hydrogen bonds, and red sticks represent the aromatic amino acids.

phenyl interactions are favorable in supramolecular structures, since the π-cloud can simultaneously interact with other entities in the vicinity.[26,27] In amyloids, the simultaneous interactions of the Phe ring are interactions with nonaromatic residues; the most frequent are interactions with the leucine side chain (Table 3).

In the example shown in Figure 9A, the Phe ring forms a parallel interaction with another Phe ring at a large offset and simultaneously interacts with leucine (Figure 9A). In strands with Tyr, the Tyr protrudes between the side chains of the opposite sheet, due to its side chain forming hydrogen bond with the opposite sheet (Figure 9B). This Tyr arrangement contributes to the relatively small range of offset values for Tyr−Tyr interactions (Figure 8).

In contrast to the intersheet interactions (see below) the intrasheet aromatic contacts do not involve C−H/O and C−H/π interactions, as there is no geometric condition for these interactions. Namely, C−H/π are impossible with small inter-ring angles (Figure 8), while the C−H/O interactions of Tyr (only Tyr possesses oxygen) are not possible for the small offsets observed in amyloid structures (Figure 8).

The interstrand hydrogen bonds of the backbone groups stabilize individual beta-sheets, and they are stronger than $\pi-\pi$ interactions.[10] Thus, the intrasheet Ar/Ar interactions are probably the consequence of the steric condition inside a protein β-sheet, although interactions between aromatic rings also contribute to the stabilization of a sheet. Examples in Figure 10 show that the antiparallel beta-sheet arrangement prevents the intrasheet Ar/Ar interactions, while the parallel arrangement results in the intrasheet interactions. In the structures where intrasheet interactions are present, they are always arranged as an array of rings. This arrangement also maximizes the intrasheet backbone hydrogen bonds between the parallel β-strands, because the strands are always aligned along the entire length, Figure 10. Also, intrasheet Ar/Ar interactions are not formed in every parallel structure (in 10 out of 36 structures interactions not formed), even when rings are aligned, which indicates poor importance of the intrasheet Ar/Ar interactions in amyloids.

Intersheet Aromatic−Aromatic Interactions. Histograms with geometric data for intersheet Ar/Ar interactions are given in Figure 11 and show significant differences between the inter- and intrasheet interaction geometries (Figure 6). In contrast to the case of intrasheet interactions, the intersheet interactions have no parallel ring arrangements; the P_1/P_2 angles for most of the interactions have values in the range 30−40° (Figure 11). The histogram with offset values has two sharp maxima, at 2.5−3.0 Å and 5.5−6.5 Å (Figure 11), while the range of offset values for intrasheet interactions is 2.5−5.0 Å (Figure 6). The intersheet interactions exhibit a somewhat larger distance (d) than the intrasheet interactions, and the Cα-Cα distance is much larger, since the rings from different sheets are pointed toward each other.

The intersheet interactions are mostly pairwise, in contrast to the intrasheet interactions, where there are several rings stacked subsequently. In order to probe the influence of aromatic ring type the angle P_1/P_2—offset dependence was obtained separately for Phe−Phe, Phe−Tyr, and Tyr−Tyr interactions, the three types of the intersheet interactions that were found in amyloid structures (Figure 12A). Like the intrasheet interactions, the mixed-type interactions are not common; however, in the intersheet interactions the Tyr−Tyr interactions prevail, while in the intrasheet the majority of interactions are Phe−Phe (Table 2).

The intersheet Ar/Ar interactions have values of geometric parameters over a large range, indicating a variety of interaction geometries. This could be the consequence of a higher ring steric freedom, as amyloid sheets are not as close as the strands inside a sheet. The interactions of two aromatic rings with inter-ring angles around zero and with offsets up to 2.0 Å had been considered as stacking interactions. Recently, Zarić and co-workers found significantly strong benzene−benzene interactions also at larger offsets, up to 5.5 Å.[26,27] Furthermore, the interactions with P_1/P_2 angles up to 40° could be

DOI: 10.1021/acs.cgd.7b01035
Cryst. Growth Des. XXXX, XXX, XXX−XXX

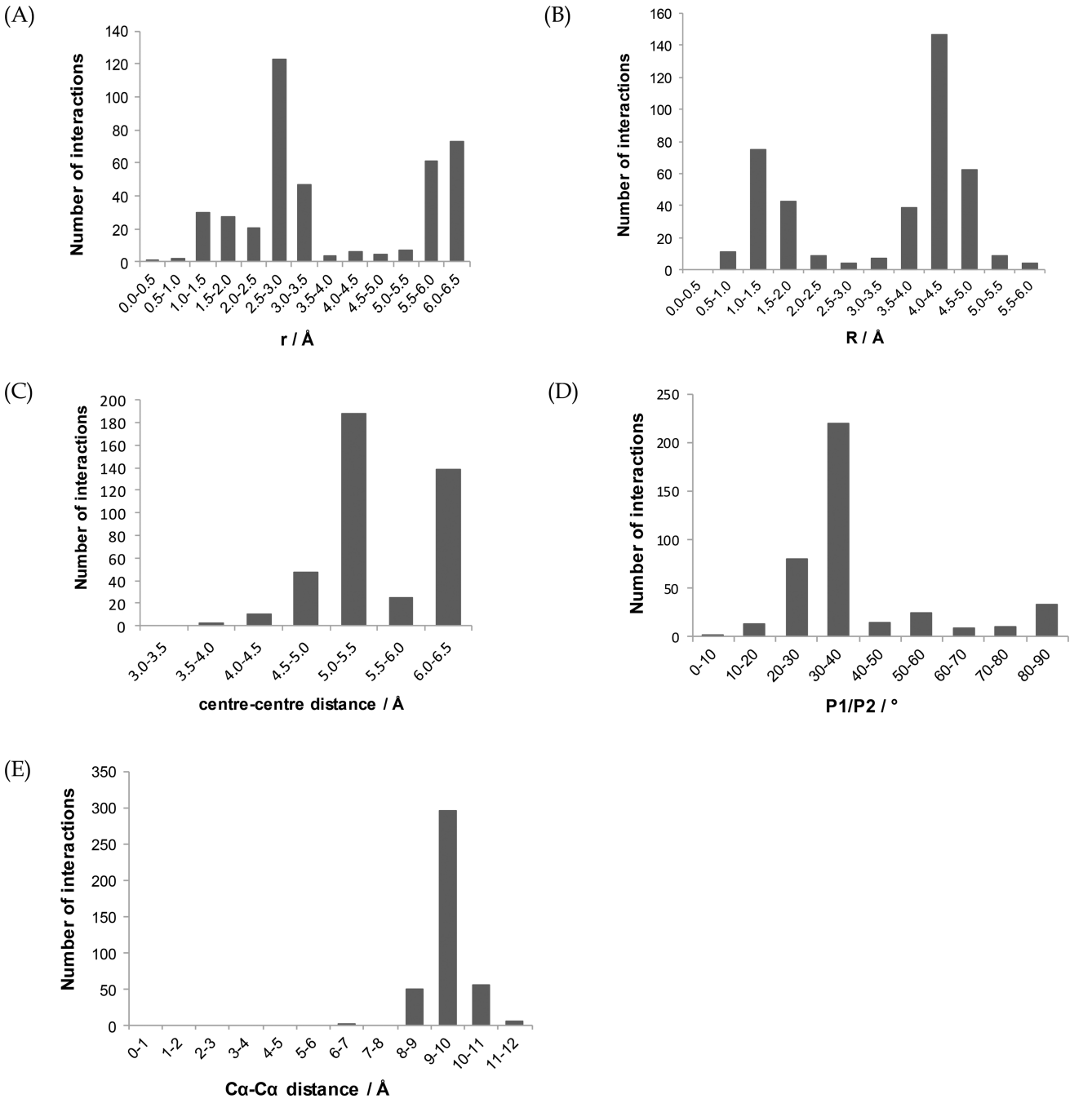

Figure 11. Geometry parameters for the intersheet aromatic−aromatic interactions: (A) Distribution of the offset values (r), (B) distribution of the normal distances (R), (C) center−center distance distribution, (D) distribution of the angles between aromatic rings, and (E) distribution of the Cα−Cα distances.

considered stacking, as they exhibit an energy-offset dependence like that in the parallel interactions.[26]

Most of the intermolecular Ar/Ar interactions are displaced stackings (Figure 12B), although they can form other types of interactions as well, like C−H/O[36,37] and C−H/π.[37] The number of C−H/O interactions is 22, and the number of C−H/π interactions is 31 (Figure 12B). The structures in Figure 13 exemplify characteristic interactions between aromatic moieties: stacking, displaced stacking, C−H/O and C−H/π interactions.

The rest, namely, the 176 "other" interactions, do not satisfy criteria for any of the interactions. However, they are all attractive. The potential surface for Ar/Ar interactions[20] shows that the interactions at offsets around 3.0 Å with P_1/P_2 angles around 50° have interaction energies close to −2.0 kcal/mol, while the interactions at offsets around 6.0 Å with P_1/P_2 angles around 30° have interaction energies between −0.5 and −1.0 kcal/mol. The vast majority (145/176) of these "other" interactions belong to a single 20-framed NMR structure, PDB ID 2M5N, as shown in Figure S3.

The geometrical parameters for the interacting rings belonging to the parallel and antiparallel strands are very similar (Figure 12C), indicating that orientation of strands does not have a significant influence on the intersheet interactions.

Aromatic−Nonaromatic Interactions. The intrasheet Ar/nAr interactions are long with no peak at lower heavy

DOI: 10.1021/acs.cgd.7b01035
Cryst. Growth Des. XXXX, XXX, XXX−XXX

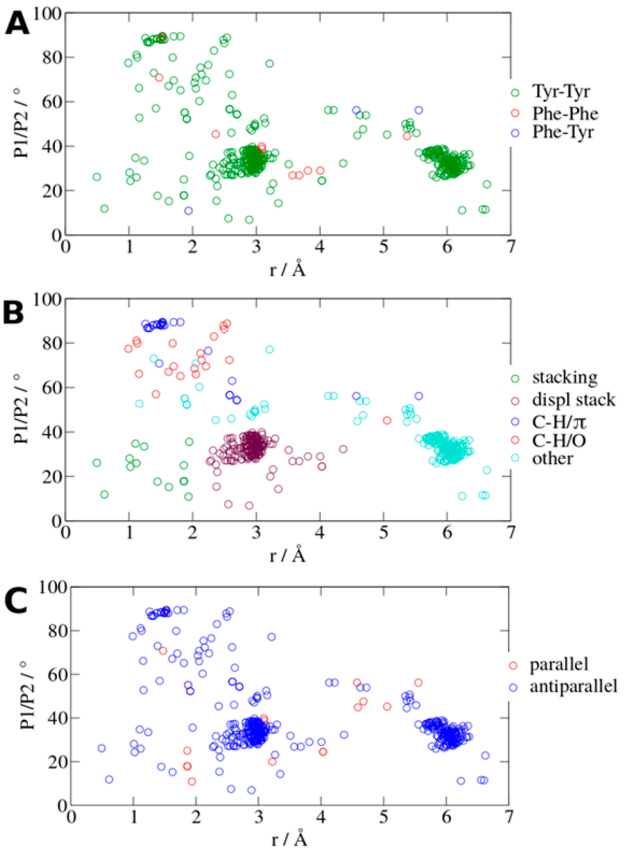

Figure 12. (A) P_1/P_2 angle-offset dependence for the intersheet aromatic−aromatic interactions. (B) Influence of the aromatic amino acid type. (C) Various types of interactions.

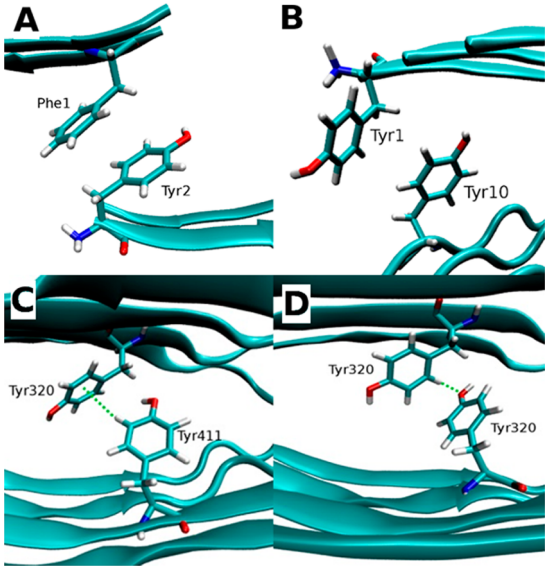

Figure 13. Representative structures of the intersheet interactions found in amyloids. (A) stacking: P_1/P_2 = 10.90°, r = 1.94 Å, PDBid 4OLR, (B) displaced stacking: P_1/P_2 = 33.78°, r = 3.02 Å, PDBid 2M5N, (C) C−H/π interactions: P_1/P_2 = 76.51°, r = 2.25 Å, PDBid 2NNT, (D) C−H/O interaction: P_1/P_2 = 79.90°, r = 1.13 Å, PDBid 2NNT. The green dotted lines represent the putative interactions.

atom−heavy atom distances between two interacting amino acids (Figure 14). Rings interact with various nonaromatic side chains with no strong preference for any side chain (Table 3).

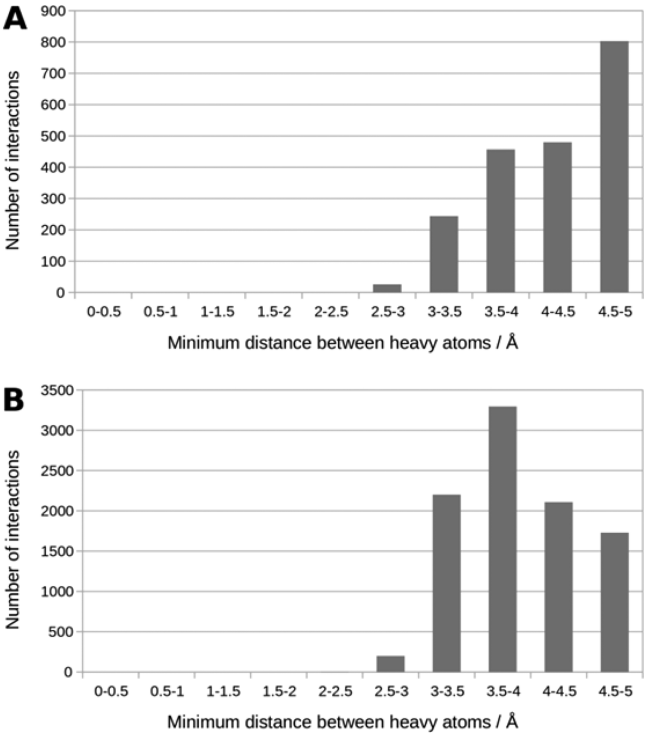

Figure 14. Histogram of minimum distances between heavy atoms of two amino acids in aromatic−nonaromatic interactions; (A) intrasheet (B) intersheet.

These intrasheet interactions could also be the result of steric conditions. The number of the interactions show that the intrasheet Ar/nAr interactions are not particularly important (Table 1).

Differently than interacting distances of Ar/nAr intrasheet interaction, the distances of intersheet interactions exhibit a peak at 3.5−4.0 Å (Figure 14B). As the nonaromatic residues are much more numerous (in average, every aromatic ring interacts with ∼3 nonaromatic, and ∼1.5 aromatic residues), we performed an analysis of the number of rings taking part in certain types of interactions: Ar/Ar or Ar/nAr. Four times higher number of aromatic rings takes part in the intersheet Ar/nAr than in the Ar/Ar interactions (3646 over 902, Table 1). The interaction energy of Ar/nAr interaction can be also substantial, comparable or even stronger than the Ar/Ar ones, as shown by the interactions energy calculations.[28] Considering particular amino acids, Phe has the highest preference toward Ar/nAr interactions, while Tyr does not have large preference for Ar/nAr interactions (Table 1).

The intersheet Ar/nAr interactions were found to involve mostly aliphatic amino acids, especially Leu and Ile (24.7% and 21.0%, Table 3). An example of the interaction between Phe and Leu is shown in Figure 9A.

Among the aromatic amino acids, phenylalanine was found to be the most frequent in these contacts.

The greater impact of the intersheet Ar/nAr over Ar/Ar interactions confirms previous experimental findings that aromatic amino acid properties other than aromaticity could be more important for amyloids, such as hydrophobicity, low chain flexibility, and β-sheet propensity.[18,21,40]

DOI: 10.1021/acs.cgd.7b01035
Cryst. Growth Des. XXXX, XXX, XXX−XXX

CONCLUSIONS

By analyzing the aromatic−aromatic interactions in amyloids in the PDB, it was established that aromatic amino acids are not present in every amyloid sequence, and thus they are not essential for amyloid self-assembly. The aromatic−aromatic interactions in amyloids are less frequent than aromatic−aliphatic interactions. In addition, the aromatic−aliphatic interactions are present in more structures than the aromatic−aromatic ones. Aromatic rings in amyloids tend much more to interact with nonaromatic residues, especially aliphatic ones, which is partially caused by a small number of aromatic and a high number of aliphatic amino acids in the amyloid sequences.

The aromatic−aromatic interactions between adjacent β-strands within the same β-sheet of an amyloid protein structure are far more frequent than the intersheet interactions. Since the aromatic−aromatic interactions are predominantly of the intrasheet type, one can conclude that they play a less dominant role for the association of amyloid sheets.

For the intrasheet aromatic−aromatic interactions, a parallel displaced geometry is the most frequent, with the P_1/P_2 interplanar angles of 0−5° and varying offset values in the range of 2.5−5.0 Å. In the case of the intersheet interactions, there are no parallel ring arrangements. The most frequent are displaced rings with P_1/P_2 interplanar angles between 30 and 40°.

ASSOCIATED CONTENT

Supporting Information

The Supporting Information is available free of charge on the ACS Publications website at DOI: 10.1021/acs.cgd.7b01035.

Figure of an example of turn and coil aromatic amino acids in amyloids (Figure S1), figure of the structure with Trp−Trp intrasheet interactions (Figure S2), and figure of the 20-framed NMR structure, PDBid 2M5N (Figure S3) (PDF)

AUTHOR INFORMATION

Corresponding Author

*Phone: 011-3336605. E-mail: szaric@chem.bg.ac.rs.

ORCID

Michael B. Hall: 0000-0003-3263-3219

Snežana D. Zarić: 0000-0002-6067-2349

Notes

The authors declare no competing financial interest.

ACKNOWLEDGMENTS

This work was supported by an NPRP grant from the Qatar National Research Fund (a member of the Qatar Foundation) [Grant Number NPRP8-425-1-087]. I.M.S. is grateful to the Serbian Ministry of Education, Science and Technological Development [Grant Number 172065] for supporting this work.

REFERENCES

(1) Laurén, J.; Gimbel, D. A.; Nygaard, H. B.; Gilbert, J. W.; Strittmatter, S. M. *Nature* **2009**, *457*, 1128−1132.

(2) Haataja, L.; Gurlo, T.; Huang, C. J.; Butler, P. C. *Endocr. Rev.* **2008**, *29*, 303−316.

(3) Ferreira, S. T.; Vieira, M. N. N.; De Felice, F. G. *IUBMB Life* **2007**, *59*, 332−345.

(4) Irvine, G. B.; El-Agnaf, O. M.; Shankar, G. M.; Walsh, D. M. *Mol. Med.* **2008**, *14*, 451−464.

(5) Murphy, M. P.; LeVine, H. *J. Alzheimer's Dis.* **2010**, *19*, 311−323.

(6) Pulawski, W.; Ghoshdastider, U.; Andrisano, V.; Filipek, S. *Appl. Biochem. Biotechnol.* **2012**, *166*, 1626−1643.

(7) Slotta, U.; Hess, S.; Spiess, K.; Stromer, T.; Serpell, L.; Scheibel, T. *Macromol. Biosci.* **2007**, *7*, 183−188.

(8) Li, C.; Mezzenga, R. *Nanoscale* **2013**, *5*, 6207−6218.

(9) Lakshmanan, A.; Cheong, D. W.; Accardo, A.; Di Fabrizio, E.; Riekel, C.; Hauser, C. A. E. *Proc. Natl. Acad. Sci. U. S. A.* **2013**, *110*, 519−524.

(10) Harrison, R. S.; Sharpe, P. C.; Singh, Y.; Fairlie, D. P. *Rev. Physiol. Biochem. Pharmacol.* **2007**, *159*, 1−77.

(11) Bowerman, C. J.; Liyanage, W.; Federation, A. J.; Nilsson, B. L. *Biomacromolecules* **2011**, *12*, 2735−2745.

(12) Cukalevski, R.; Boland, B.; Frohm, B.; Thulin, E.; Walsh, D.; Linse, S. *ACS Chem. Neurosci.* **2012**, *3*, 1008−1016.

(13) Doran, T. M.; Kamens, A. J.; Byrnes, N. K.; Nilsson, B. L. *Proteins: Struct., Funct., Genet.* **2012**, *80*, 1053−1065.

(14) Milardi, D.; Sciacca, M. F. M.; Pappalardo, M.; Grasso, D. M.; La Rosa, C. *Eur. Biophys. J.* **2011**, *40*, 1−12.

(15) Tu, L.-H.; Raleigh, D. P. *Biochemistry* **2013**, *52*, 333−342.

(16) Azriel, R.; Gazit, E. *J. Biol. Chem.* **2001**, *276*, 34156−34161.

(17) Görbitz, C. H. *Chem. Commun.* **2006**, No. No. 22, 2332−2334.

(18) Lee, N. R.; Bowerman, C. J.; Nilsson, B. L. *Biomacromolecules* **2013**, *14*, 3267−3277.

(19) Qi, R.; Luo, Y.; Ma, B.; Nussinov, R.; Wei, G. *Biomacromolecules* **2014**, *15*, 122−131.

(20) Profit, A. A.; Vedad, J.; Saleh, M.; Desamero, R. Z. B. *Arch. Biochem. Biophys.* **2015**, *567*, 46−58.

(21) Bemporad, F.; Taddei, N.; Stefani, M.; Chiti, F. *Protein Sci.* **2006**, *15*, 862−870.

(22) Profit, A. A.; Felsen, V.; Chinwong, J.; Mojica, E.-R. E.; Desamero, R. Z. B. *Proteins: Struct., Funct., Genet.* **2013**, *81*, 690−703.

(23) Gazit, E. *FASEB J.* **2002**, *16*, 77−83.

(24) Anjana, R.; Vaishnavi, M. K.; Sherlin, D.; Kumar, S. P.; Naveen, K.; Kanth, P. S.; Sekar, K. *Bioinformation* **2012**, *8*, 1220−1224.

(25) Chourasia, M.; Sastry, G. M.; Sastry, G. N. *Int. J. Biol. Macromol.* **2011**, *48* (4), 540−552.

(26) Ninković, D. B.; Andrić, J. M.; Malkov, S. N.; Zarić, S. D. *Phys. Chem. Chem. Phys.* **2014**, *16*, 11173−11177.

(27) Ninković, D. B.; Janjić, G. V.; Veljković, D. Ž.; Sredojević, D. N.; Zarić, S. D. *ChemPhysChem* **2011**, *12*, 3511−3514.

(28) Ninković, D. B.; Malenov, D. P.; Petrović, P. V.; Brothers, E. N.; Niu, S.; Hall, M. B.; Belić, M. R.; Zarić, S. D. *Chem. - Eur. J.* **2017**, *23*, 11046.

(29) Ninković, D. B.; Vojislavljević-Vasilev, D. Z.; Medaković, V. B.; Hall, M. B.; Brothers, E. N.; Zarić, S. D. *Phys. Chem. Chem. Phys.* **2016**, *18*, 25791−25795.

(30) Bowerman, C. J.; Ryan, D. M.; Nissan, D. A.; Nilsson, B. L. *Mol. BioSyst.* **2009**, *5*, 1058−1069.

(31) Berman, H. M.; Westbrook, J.; Feng, Z.; Gilliland, G.; Bhat, T. N.; Weissig, H.; Shindyalov, I. N.; Bourne, P. E. *Nucleic Acids Res.* **2000**, *28*, 235−242.

(32) Allen, F. H. *Acta Crystallogr., Sect. B: Struct. Sci.* **2002**, *58*, 380−388.

(33) Stanković, I.; Hall, M. B.; Zarić, S. D. *Trans. Internet Res.* **2017**, *13*.

(34) Michaud-Agrawal, N.; Denning, E. J.; Woolf, T. B.; Beckstein, O. *J. Comput. Chem.* **2011**, *32*, 2319−2327.

(35) Dragelj, J. L.; Stanković, I. M.; Božinovski, D. M.; Meyer, T.; Veljković, D. Z.; Medaković, V. B.; Knapp, E. W.; Zarić, S. D. *Cryst. Growth Des.* **2016**, *16*, 1948−1957.

(36) Veljković, D. Ž.; Janjić, G. V.; Zarić, S. D. *CrystEngComm* **2011**, *13*, 5005.

(37) Milčić, M. K.; Medaković, V. B.; Sredojević, D. N.; Juranić, N. O.; Zarić, S. D. *Inorg. Chem.* **2006**, *45*, 4755−4763.

(38) MacKerell, A. D. J.; Bashford, D.; Bellott, M.; Dunbrack, R. L.; Evanseck, J. D.; Field, M. J.; Fischer, S.; Gao, J.; Guo, H.; Ha, S.;

DOI: 10.1021/acs.cgd.7b01035
Cryst. Growth Des. XXXX, XXX, XXX−XXX

545 Joseph-McCarthy, D.; Kuchnir, L.; Kuczera, K.; Lau, F. T. K.; Mattos,
546 C.; Michnick, S.; Ngo, T.; Nguyen, D. T.; et al. *J. Phys. Chem. B* **1998**,
547 *102*, 3586−3616.
548 (39) Apweiler, R.; Bairoch, A.; Wu, C. H.; Barker, W. C.;
549 Boeckmann, B.; Ferro, S.; Gasteiger, E.; Huang, H.; Lopez, R.;
550 Magrane, M.; Martin, M. J.; Natale, D. A.; O'Donovan, C.; Redaschi,
551 N.; Yeh, L.-S. L. *Nucleic Acids Res.* **2004**, *32*, 115D−119.
552 (40) Senguen, F. T.; Lee, N. R.; Gu, X.; Ryan, D. M.; Doran, T. M.;
553 Anderson, E. A.; Nilsson, B. L. *Mol. BioSyst.* **2011**, *7*, 486−496.

DOI: 10.1021/acs.cgd.7b01035
Cryst. Growth Des. XXXX, XXX, XXX−XXX